forests

MDPI

Article

Mechanism-Driven Adaptive Combined Inversion of Forest Height Using P-Band PolInSAR Data

Feifei Dai [1], Wangfei Zhang [2], Yongjie Ji [1,*] and Han Zhao [2]

[1] College of Soil and Water Conservation, Southwest Forestry University, Kunming 650224, China
[2] College of Forestry, Southwest Forestry University, Kunming 650224, China
* Correspondence: jiyongjie@live.cn

Abstract

Forest height is a key parameter for quantifying forest biomass and carbon stocks and serves as an important indicator of forest ecosystem health. The successful launch of the European Space Agency's P-band Biomass satellite, which provides Polarimetric Interferometric Synthetic Aperture Radar (PolInSAR) data for global high-precision forest height mapping, heralds a new era in global forest carbon monitoring. However, the accuracy of forest height inversion is significantly influenced by scattering mechanisms. This study investigates the impact of dominant scattering mechanisms on forest height inversion accuracy. Four classical algorithms were selected: the polarimetric phase center height estimation method (PPC), the complex coherence phase center differencing algorithm (CCPCD), the coherence amplitude inversion method (CAI), and the hybrid inversion method using both phase and coherence information. The Freeman–Durden three-component decomposition was employed to identify the dominant scattering mechanisms. The results show that (1) at P-band, inversion model performance exhibits strong coupling with scattering mechanisms, and no single algorithm achieves global robustness; (2) the hybrid inversion method using both phase and coherence information performs better in regions dominated by surface and double-bounce scattering, whereas the coherence amplitude inversion method (CAI) yields higher accuracy in volume-scattering-dominated regions; and (3) the adaptive joint inversion strategy based on scattering mechanisms achieved a root mean square error (RMSE) of 4.62 m and a coefficient of determination (R^2) of 0.76 at P-band, representing an improvement of approximately 30% over the best single-model performance (RMSE = 6.51 m). This approach overcomes the accuracy limitations of single models in complex global forest scenarios and provides a valuable reference for scientific forest height inversion.

Keywords: P-band PolInSAR; forest height inversion; scattering mechanisms; combined inversion

Check for updates

Academic Editor: Rafael María Navarro-Cerrillo

Received: 31 January 2026
Revised: 9 March 2026
Accepted: 13 March 2026
Published: 16 March 2026

Copyright: © 2026 by the authors. Licensee MDPI, Basel, Switzerland. This article is an open access article distributed under the terms and conditions of the Creative Commons Attribution (CC BY) license.

1. Introduction

Forests, as a vital component of terrestrial ecosystems, play essential roles in climate regulation, carbon sequestration, hydrological cycling, and biodiversity maintenance, thereby contributing to global ecological balance and sustainable human development [1]. Forest height serves as a key indicator of forest ecosystem health and ecological functions and constitutes a core parameter for quantifying forest biomass and carbon stocks [2]. However, optical remote sensing, owing to its short wavelengths, struggles to penetrate the forest canopy and is highly susceptible to interference from clouds and fog, limiting its ability to retrieve vertical forest structure information. In contrast, Light Detection and Ranging

(LiDAR) technology enables the relatively precise acquisition of forest height information, but its discrete point- or strip-based sampling hinders seamless image coverage without integration with other data sources [3–5]. Polarimetric Interferometric Synthetic Aperture Radar (PolInSAR) technology integrates the high sensitivity of Polarimetric Synthetic Aperture Radar (PolSAR) to scatterer shape, orientation, and dielectric properties with the capability of Interferometric Synthetic Aperture Radar (InSAR) to resolve vegetation vertical structure and height distributions, offering robust support for the remote sensing inversion of forest parameters [6,7].

The successful launch of the European Space Agency's P-band Biomass satellite represents a significant advancement in global forest carbon stock monitoring. The longer wavelength of P-band enables deeper penetration into the forest canopy, resulting in enhanced ground echo visibility compared to shorter-wavelength bands. Kumar et al. [8] reported that P-band PolInSAR data, when processed with the Random Volume over Ground (RVoG) model, achieved root mean square errors (RMSE) of 1–2 m for canopy height inversion in dense tropical forests. In recent years, PolInSAR technology has been widely applied to invert forest parameters such as height, above-ground biomass, and underlying topography, yielding substantial progress [9–11]. For instance, Liu et al. [12] utilized airborne P-band Tomographic SAR (TomoSAR) data to jointly estimate forest height and above-ground biomass in the Lopé and Mondah regions of Gabon; their results demonstrated the high sensitivity of P-band TomoSAR to tropical forest vertical structure and strong potential for biomass estimation. Xie et al. [13] proposed a multi-baseline inversion scheme adapted to low signal-to-noise ratio conditions by fusing P-band SAR data from the F-SAR and ONERA SETHI systems, achieving forest height extraction accuracy within an RMSE of 2.37 m.

Current tree height inversion methods can generally be classified into four categories: (1) phase-difference-based methods that estimate tree height from the vegetation scattering phase center, such as the DSM–DEM differencing approach [14]; (2) scattering model-based methods, with the Random Volume over Ground (RVoG) model—built on random volume coherence—being the most widely used [15]; (3) coherence amplitude inversion methods, which estimate forest height by constructing the complex coherence matrix of the scattering vector to separate canopy and ground contributions and exploit amplitude information [16,17]; and (4) hybrid inversion methods that integrate both phase and coherence information for forest height retrieval [18]. Several studies have compared and refined these inversion approaches. Chen et al. [19] systematically evaluated the performance of the DEM differencing algorithm, coherence amplitude inversion, hybrid phase-coherence inversion, and three-stage RVoG inversion, concluding that the three-stage RVoG algorithm provided the highest accuracy when accounting for coherence and terrain slope effects. Yadav et al. [20] applied TanDEM-X data for biomass inversion in Indian tropical forests, obtaining an R^2 of 0.79 and RMSE of 1.66 m. Sui et al. [21] developed a hybrid iterative optimization model that incorporates terrain-corrected incidence angle and vertical wavenumber, validated effectively on BioSAR 2008 L-band data under varying forest density conditions.

However, although existing studies have explored various RVoG-based PolInSAR inversion methods, most research remains limited to the local improvement and optimization of individual inversion algorithms. There is still a lack of systematic analysis regarding the intrinsic dependence between the four classical inversion algorithms and the dominant scattering mechanisms, which limits the robustness of these algorithms under complex forest structures. Furthermore, within the RVoG-based inversion framework, the majority of multi-model fusion strategies rely on empirical weighting or error minimization methods. These approaches typically assign static weights globally, failing to account for the

dynamic variations in scattering mechanisms across the entire remote sensing image. Moreover, since current forest height estimation methods are predominantly formulated based on forest scattering characteristics, variations in scattering mechanisms within the forest will directly impact the inversion accuracy of the selected models. Different mechanisms can lead to substantial variations in the applicability and performance of each method. Moreover, forests often exhibit mixed scattering contributions, rendering single-method approaches inadequate for maintaining consistent global accuracy. Therefore, elucidating the relationships between inversion models and dominant scattering mechanisms is crucial for enhancing global forest height inversion accuracy and developing adaptive algorithm selection strategies. To bridge this gap, this study proposes a novel adaptive combined inversion strategy. Unlike previous empirical fusion approaches, the adaptive combined inversion strategy utilized in this paper selects the inversion model based on the variations in dominant scattering mechanisms within the image. This transforms traditional empirical or weight-based fusion inversion methods into an adaptive joint inversion driven by dominant scattering mechanisms.

In forest height inversion, the complexity of forest structures leads to significant heterogeneity in scattering mechanisms within forested areas, which inevitably causes traditional single algorithms to produce large regional deviations. To address this issue, this study proposes a mechanism-driven adaptive combined inversion framework. This framework integrates Freeman–Durden polarimetric decomposition with four classical inversion algorithms for the first time, aiming to provide a scientific framework for improving the global accuracy of forest height inversion from remote sensing imagery, and to serve as a reference for future research on forest parameter inversion. To achieve this purpose, the specific research objectives of this study are as follows. Firstly, by performing Freeman–Durden polarimetric decomposition on P-band PolInSAR simulated data, data samples dominated by different scattering mechanisms are identified. Subsequently, four classical inversion models (i.e., the polarimetric phase center height estimation method, the complex coherence phase center difference method, the complex coherence amplitude inversion method, and the joint coherence amplitude and phase inversion method) are, respectively, applied to the data characterized by different dominant scattering mechanisms, in order to systematically evaluate the inversion accuracy and performance of each method under various scattering conditions. Meanwhile, real BioSAR data are utilized to verify the conclusions drawn from the simulated data and to assess the practical applicability and transferability of these conclusions. Finally, on this basis, the feasibility and advantages of the multi-model joint inversion strategy driven by dominant scattering mechanisms are explored and demonstrated.

2. Forest Scene Simulation and Real Data

2.1. Forest Scene Simulated Data Generation and Pre-Processing

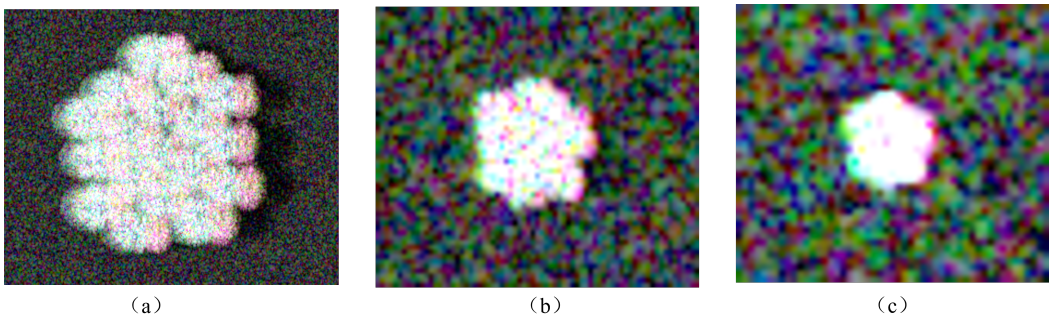
This study utilizes the PolSARpro Sim module to generate simulated P-band PolInSAR forest scenes. PolSARpro Sim is a simulation tool for generating InSAR data, developed by Dr. Mark L. Williams and integrated within the PolSARpro (Polarimetric SAR Data Processing and Educational Tool) software suite released by the European Space Agency (ESA) [14,22]. The key parameters configured in this study are presented in Table 1, including platform parameters, radar system parameters, forest scene parameters, and forest biophysical parameters.

Existing studies have shown that variations in SAR image resolution lead to significant differences in scattering mechanisms within individual pixels [21]. Accordingly, this study adopts a multi-resolution simulation approach, using the PolSARpro Sim module to generate simulated P-band PolInSAR data at varying resolutions, thereby producing

scenes dominated by different scattering mechanisms. Given that SAR systems employ side-looking imaging, ground range resolution and slant range resolution are related by the equation where is the ground range resolution, is the slant range resolution, and is the radar incidence angle [23]. Therefore, by changing the slant range resolution and the incidence angle, simulated SAR data with different ground range resolutions can be obtained, thereby yielding simulated scenes under conditions dominated by different scattering mechanisms. The Pauli RGB composite images at some representative resolutions and the corresponding forest position schematic diagrams are shown in Figures 1 and 2, respectively.

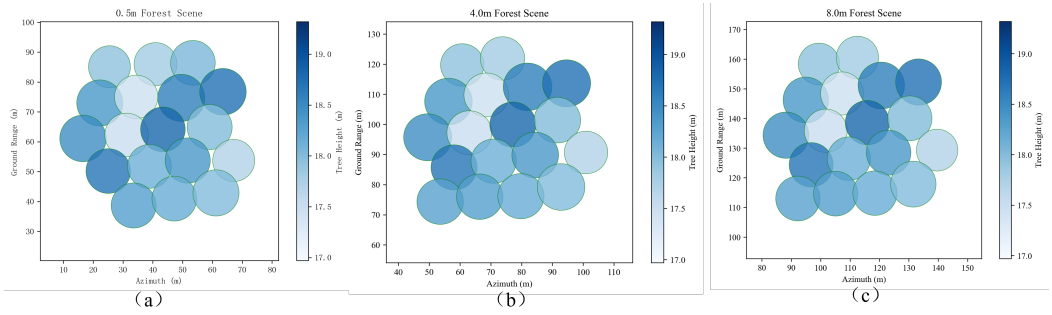
Table 1. Parameter Settings in the PolSARpro Sim Simulator.

	Type	Parameter
Platform Parameters	Platform Altitude (m)	3000
	Radar Incidence Angle (deg)	45°
	Vertical Baseline (m)	−6.0
	Horizontal Baseline (m)	6.0
Radar System Parameters	Center Frequency (GHz)	0.65
Forest Scene Parameters	Azimuth Slope (%)	0
	Range Slope (%)	0
	Surface Roughness (%)	0
	Soil Moisture (%)	0
Forest Characteristic Parameters	Average Tree Height (m)	18
	Forest Area (ha)	0.282745
	Forest Density	66



（a） （b） （c）

Figure 1. Pauli RGB composite images at different resolutions in P-band: (**a**) 0.5 m; (**b**) 4.0 m; (**c**) 8.0 m.



（a） （b） （c）

Figure 2. Forest position maps at different resolutions in P-band: (**a**) 0.5 m; (**b**) 4.0 m; (**c**) 8.0 m.

The simulated data generated by PolSARpro Sim exhibit ideal conditions, including automatic co-registration of master and slave images with one-to-one pixel correspondence and the complete absence of speckle noise. Consequently, no additional geometric registration, multi-looking, speckle filtering, or geocoding is required during data processing. This simplified workflow enables a focused evaluation of inversion model performance by isolating the effects of the methods themselves from external factors such as noise suppression.

Leveraging these data characteristics, this study applies Freeman–Durden three-component decomposition to the simulated data across different resolutions. By examining the relative contributions of surface, double-bounce, and volume scattering components at varying resolutions, simulated scenes dominated by different scattering mechanisms are identified. Simulated images at the corresponding resolutions are then selected for subsequent inversion based on the dominant scattering mechanism. The interferometric processing workflow for the simulated data consists of three main steps: (1) generation of raw interferometric phase maps; (2) flat-earth phase removal to produce flattened interferometric phase maps; and (3) generation of interferometric coherence maps. These steps extract the essential interferometric features required for inversion. The detailed processing workflow is described in Ref. [24].

2.2. Acquisition and Pre-Processing of Real-World Forest Scene Data

(1) Overview of the Study Area

The study area is located in the forested region of the Krycklan catchment, Vindeln Municipality, Västerbotten County, northern Sweden. A schematic overview of the study area is presented in Figure 3. The terrain is predominantly hilly with moderate slopes, whereas the forest canopy exhibits relatively uniform height with minimal variation. The dominant forest types are coniferous and broadleaf forests. The primary tree species in coniferous stands are Scots pine (*Pinus sylvestris*) and Norway spruce (*Picea abies*), while birch (*Betula* spp.) predominates in broadleaf forests [14].

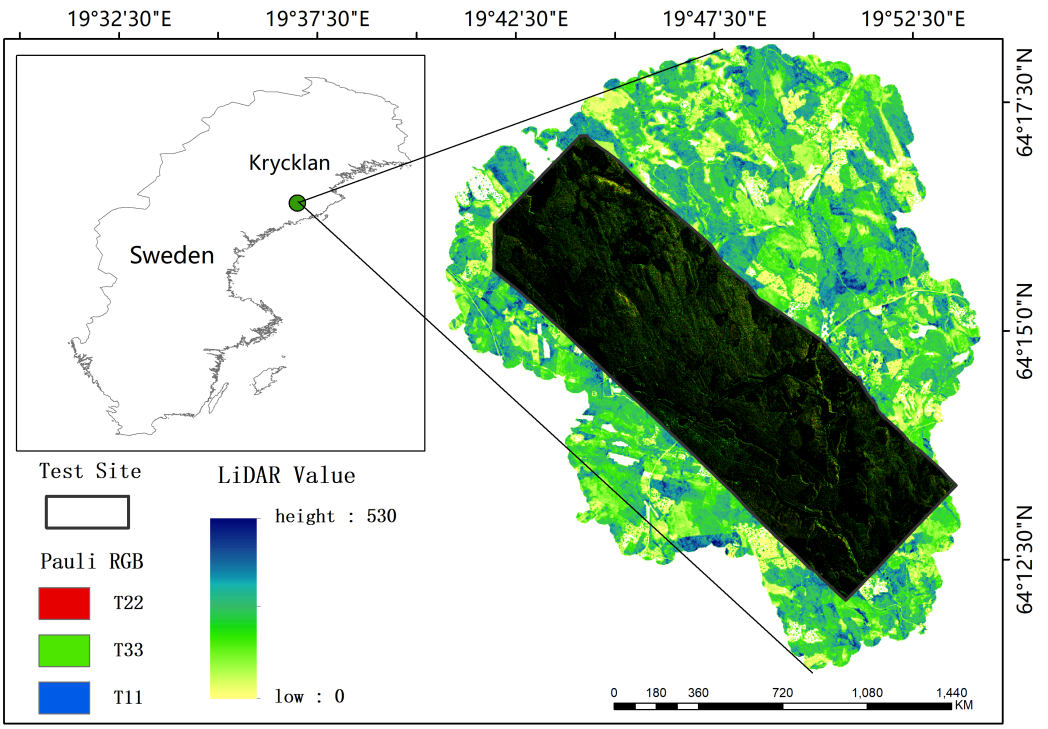


Figure 3. Overview of the study area.

(2) Data Acquisition and Pre-processing

The PolInSAR data used in this study were acquired during the BioSAR 2008 campaign over the Krycklan catchment, Sweden, in October 2008. The data were collected by the German Aerospace Center (Deutsches Zentrum für Luft- und Raumfahrt, DLR) and the Swedish Defence Research Agency (FOI) using the airborne E-SAR system [14,18]. The P-band PolInSAR dataset includes corresponding slave images paired with a single master image, enabling robust forest height inversion and scattering mechanism identification.

Additionally, the BioSAR 2008 campaign acquired high-resolution airborne LiDAR data over the same area, with a point density yielding a spatial resolution of 0.5 m. The LiDAR data were collected in late summer 2008, ensuring temporal consistency with the PolInSAR acquisitions. In this study, the LiDAR-derived forest height serves as the reference ground truth. Comparison with inversion results from various models enables quantitative evaluation of accuracy and bias under different dominant scattering mechanisms, providing a basis for selecting optimal models and validating the proposed joint inversion strategy.

The acquired PolInSAR single-look complex (SLC) images are pre-registered at the sub-pixel level, eliminating the need for additional geometric co-registration. Data processing proceeds as follows. First, a 3 × 1 (azimuth × range) multi-look operation is applied to reduce speckle noise and enhance image quality. Second, Freeman–Durden three-component decomposition is performed on the multi-looked data, separating forest scattering into surface (odd-bounce), double-bounce, and volume scattering contributions. Analysis of their relative powers identifies dominant scattering mechanisms at different spatial locations, providing a physical foundation for subsequent model optimization. In the interferometric processing stage, interferometric phase estimation, flat-earth phase removal, adaptive filtering, and complex coherence estimation are sequentially applied to generate high-quality interferometric products. Four classical forest height inversion models are then employed to estimate height distributions in the radar geometry. Finally, geocoding transforms the inverted height maps from radar to geographic coordinates, enabling spatial alignment with LiDAR reference data for accuracy assessment.

3. Research Methodology

3.1. Overview of the Methodology

In this study, Freeman–Durden three-component decomposition was applied to both the simulated data and the real airborne PolInSAR data to obtain the surface scattering (F_{Odd}), double-bounce scattering (F_{Dbl}), and volume scattering (F_{Vol}) power components for each pixel. Based on the maximum power criterion, the polarimetric component with the highest power was defined as the dominant scattering mechanism of the given pixel. After identifying the dominant scattering mechanism for each pixel, a mapping relationship between the dominant mechanism and a specific inversion algorithm was established. Specifically, this study first systematically evaluated the error characteristics and applicability of four classical inversion models (i.e., the polarimetric phase center height estimation method, the complex coherence phase center difference algorithm, the coherence amplitude inversion method, and the hybrid inversion method using both phase and coherence information) under different scattering conditions. Based on the evaluation results, the optimal inversion model demonstrating the best performance under each dominant scattering mechanism was assigned. Finally, in the global inversion stage of the remote sensing image, the optimal inversion model was adaptively invoked based on the identified dominant scattering mechanism of each pixel to perform the fusion inversion, thereby improving the forest height inversion accuracy. Figure 4 illustrates the technical flowchart of the proposed methodology.

Figure 5 further details the specific decision-rule flowchart of the proposed adaptive combined inversion strategy. For the input PolInSAR data, the procedure performs Freeman–Durden decomposition on a per-pixel basis, extracting the corresponding surface scattering (F_{odd}), double-bounce scattering (F_{Dbl}), and volume scattering (F_{vol}) power components. Subsequently, by evaluating the maximum power criterion ($P_{\max}$), the algorithm accurately directs each pixel to the specific algorithm selection branch corresponding to its dominant scattering mechanism. Following the assignment of the optimal algorithm, the corresponding inversion is executed to derive the specific tree height (H_s, H_v, or H_d), and the calculated value is stored

back into the respective pixel. Through the continuous iteration of this rule across all pixels, a high-precision, adaptive global forest height map is ultimately generated.

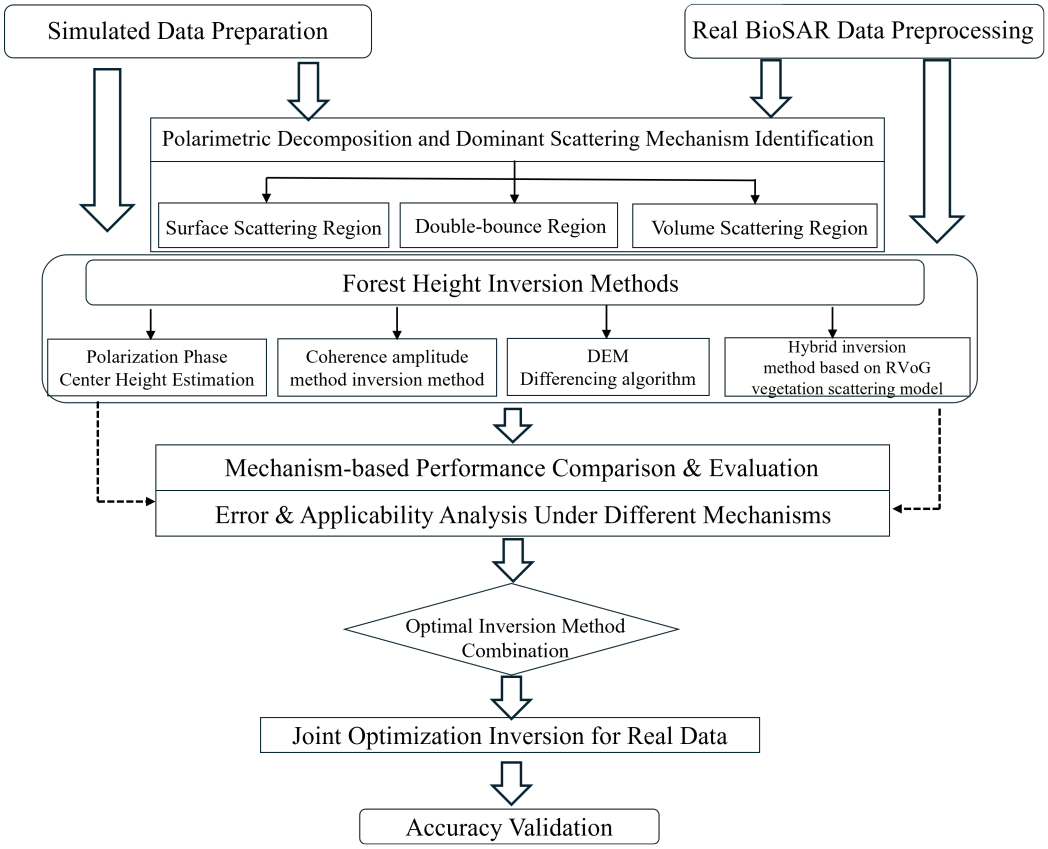


Figure 4. Technical flowchart.

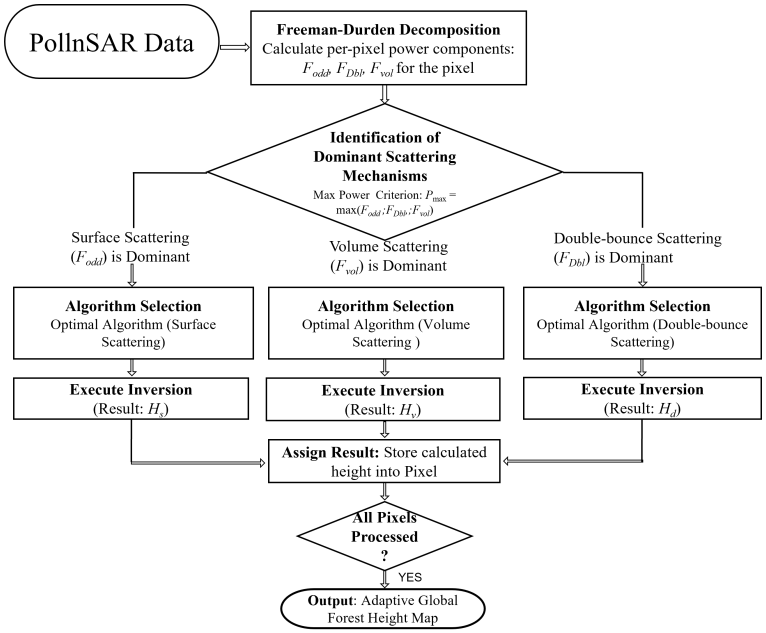


Figure 5. Flowchart of the adaptive decision-making process.

3.2. Freeman–Durden Three-Component Polarimetric Decomposition Method

The Freeman–Durden three-component decomposition, based on a three-scattering-mechanism model and the reflection symmetry assumption, separates the polarimetric

covariance matrix into surface (odd-bounce), double-bounce, and volume scattering contributions. These components correspond to the primary scattering mechanisms in forest scenes, providing a physical foundation for identifying dominant scattering mechanisms and selecting appropriate inversion models [25].

In the Freeman–Durden three-component decomposition, the surface scattering component models first-order Bragg scattering from slightly rough surfaces (denoted F_Odd). This component represents odd-bounce scattering, primarily from ground or canopy surfaces, and its contribution to the polarimetric covariance matrix is given by Equation (1).

$$T_s = \begin{bmatrix} 1 & \beta^* & 0 \\ \beta & |\beta|^2 & 0 \\ 0 & 0 & 0 \end{bmatrix}; \quad \beta = \frac{R_H - R_V}{R_H + R_V} \tag{1}$$

Here, T_s represents the surface scattering component, and R_H and R_V are the reflection coefficients for horizontal and vertical polarizations, respectively, as shown in Equations (2) and (3):

$$R_H = \frac{\cos\theta - \sqrt{\varepsilon_r - \sin^2\theta}}{\cos\theta + \sqrt{\varepsilon_r - \sin^2\theta}} \tag{2}$$

$$R_V = \frac{(\varepsilon_r - 1)\{\sin^2\theta - \varepsilon_r(1 + \sin^2\theta)\}}{\left(\varepsilon_r \cos\theta + \sqrt{\varepsilon_r - \sin^2\theta}\right)^2} \tag{3}$$

where θ is the local incidence angle, and ε_r is the relative dielectric constant of the rough surface. This component characterizes the direct single scattering from the forest canopy or the ground surface, representing a single reflection of electromagnetic waves by the forest surface. In forest height inversion, the surface scattering component can serve as a baseline reference for the forest signal echo height, used to determine the upper boundary of the vegetation canopy.

The second component is the double-bounce scattering (denoted as F_Dbl), and its scattering model can be expressed as Equation (4):

$$T_d = \begin{bmatrix} |\alpha|^2 & \alpha & 0 \\ \alpha^* & 1 & 0 \\ 0 & 0 & 0 \end{bmatrix}; \quad \alpha = \frac{e^{j\gamma_V} R_{TH} R_{GH} + e^{j\gamma_H} R_{TV} R_{GV}}{e^{j\gamma_V} R_{TH} R_{GH} - e^{j\gamma_H} R_{TV} R_{GV}} \tag{4}$$

In the equation, T_d represents the double-bounce scattering component; R_{TH} and R_{TV} are the reflection coefficients of the vertical trunk surface for horizontal and vertical polarizations, respectively; R_{GH} and R_{GV} represent the Fresnel reflection coefficients of the horizontal ground, respectively; and $e^{j\gamma_H}$ and $e^{j\gamma_V}$ are the propagation factors, where γ_H and γ_V are the influences of attenuation and phase change during the process of electromagnetic wave propagation. This component describes the double-bounce scattering between the tree trunks and the ground in the forest, representing the multiple reflections of electromagnetic waves through the trunk–ground interface. However, in dense forests, due to the strong attenuation effect of the canopy on electromagnetic waves, the ability of the signal to penetrate to the trunk–ground interface is limited. Therefore, the double-bounce scattering component is usually relatively weak in actual forest scenes, and this characteristic is particularly obvious in short-wavelength PolInSAR data. But in special spaces such as sparse woodlands, the canopy density is low, and double-bounce scattering may still occupy a dominant position. Therefore, evaluating the inversion performance of different inversion models under the conditions dominated by double-bounce scattering also has important guiding significance for the height inversion of such special forest land surfaces.

The third component, the volume scattering component (F_Vol), is represented by T_v in the equation. This component characterizes the forest canopy as a cloud of scatterers composed of randomly oriented dipoles, used to describe the scattering from within the forest canopy in forest scenes. The volume scattering model describes the characteristics of completely random dipoles [26–29]. Its final volume scattering model can be expressed as Equation (5):

$$T_v = \begin{bmatrix} 2 & 0 & 0 \\ 0 & 1 & 0 \\ 0 & 0 & 1 \end{bmatrix} \tag{5}$$

The volume scattering component mainly originates from the complex scattering interactions within the canopy, including multiple scattering from microscopic structures such as leaves and twigs. In areas with complex forest structures, this scattering usually occupies a dominant position.

The Freeman–Durden three-component decomposition assumes that the surface, double-bounce, and volume scattering contributions are uncorrelated. Accordingly, the observed polarimetric covariance matrix is modeled as the sum of these independent contributions, expressed as Equation (6):

$$T_3 = f_s T_s + f_d T_d + f_v T_v \tag{6}$$

where f_s, f_d and f_v are the weights of surface scattering, double-bounce scattering, and volume scattering, respectively; their relative magnitudes reflect the contribution levels of each scattering mechanism to the total scattering power [25–28,30]. In this study, the dominant scattering mechanism analysis of forest PolInSAR images is conducted using the Freeman–Durden decomposition method. Specifically, by calculating the weights or relative contributions of each scattering component, the types of dominant scattering mechanisms (surface scattering dominant, double-bounce scattering dominant, or volume scattering dominant) at different spatial locations are identified. Based on the identified dominant scattering mechanisms, the selection of subsequent forest height inversion methods is guided, and the coupling relationship between forest dominant scattering mechanisms and inversion models is explored. This provides a scientific basis for the determination of the optimal inversion model and the improvement of the accuracy of the subsequent fusion inversion method.

3.3. Forest Height Inversion Algorithms

Based on the different principles adopted in forest height estimation, the inversion methods can be categorized into two types. The first type consists of phase center estimation methods based on the principle of interferometry, which estimate the forest canopy height by utilizing the phase centers of different polarization states, including Polarimetric phase center height estimation method and Complex coherence phase center differencing algorithm. The second type consists of quantitative inversion methods based on vegetation scattering models including the coherence amplitude inversion method and the hybrid inversion method, which quantitatively invert forest height by establishing forest scattering models using both phase and coherence information [17]. The polarimetric phase center height estimation method directly utilizes the corresponding polarization phase center of the tree crown to represent the forest canopy height, and its mathematical expression is as follows:

$$h_v = \frac{\arg(\tilde{\gamma}_{w_v})}{k_z}; \quad k_z = \frac{4\pi\Delta\theta}{\lambda \sin\theta} \approx \frac{4\pi B_\perp}{\lambda R \sin\theta} \tag{7}$$

where h_v is the estimated forest canopy height, w_v is the forest canopy scattering mechanism, $\tilde{\gamma}_{w_v}$ is the complex coherence coefficient of w_v, k_z is the effective vertical wavenumber, θ is the radar incidence angle, λ is the incident wavelength of the radar signal, $B_\perp$ is the perpendicular baseline, and R is the slant range. The complex coherence phase center differencing algorithm synthesizes different polarization states in multiple polarization channels to respectively extract the phase center representing canopy volume scattering and the phase center representing surface scattering, and then performs a differentiation calculation between the two to estimate the forest height [29]. Its mathematical expression is

$$h_v = \frac{\arg(\tilde{\gamma}_{w_v}) - \arg(\tilde{\gamma}_{w_s})}{k_z} \tag{8}$$

In this equation, w_s is the surface scattering mechanism, $\tilde{\gamma}_{w_s}$ is the complex coherence coefficient of the surface scattering mechanism, and the remaining parameters have the same meanings as those in the Polarimetric phase center height estimation method. By separating the phase centers of volume scattering and surface scattering, this method, compared to the method solely utilizing the canopy phase, improves the adaptability to complex scattering environments to a certain extent.

The coherence amplitude inversion method (also known as the SINC model method) utilizes only coherence information for forest height inversion. This method assumes that the attenuation factor is 0 and does not consider the influence of surface scattering; thus, in the case where the effective vertical wavenumber (k_z) is known, the forest height can be inverted [14]. Its mathematical expression is

$$h_v = \frac{2\pi}{k_z}\left(1 - \frac{2 \cdot \sin^{-1}(|\gamma_v|^{0.8})}{\pi}\right); \quad \gamma_v \approx e^{i(\frac{k_z h_v}{2} + \phi)} \frac{\sin\left(\frac{k_z h_v}{2}\right)}{\frac{k_z h_v}{2}} \tag{9}$$

where γ_v is the forest volume scattering complex coherence, ϕ is the surface phase, and i is the complex symbol. The advantage of this method lies in the fact that it does not rely on the accurate positioning of the phase center, but directly utilizes the coherence for height inversion; therefore, the requirements for phase unwrapping are relatively low.

Although the inversion methods based on phase difference are relatively simple to implement, their estimation accuracy highly depends on the accurate extraction of the scattering phase center of the forest canopy. Meanwhile, due to the limitations of model assumptions, there is uncertainty in the position of the inverted phase center, which may be located anywhere within the canopy height range; this often leads to an underestimation of the forest height. To overcome this limitation, Cloude et al. [26] proposed conducting forest height inversion by combining the SINC model to improve the accuracy of the estimation of forest height [15,17], which is a hybrid inversion method using both phase and coherence information. This inversion method comprehensively utilizes both phase and amplitude information to jointly invert the forest height, and its mathematical expression is

$$h_v = \frac{\arg(\tilde{\gamma}_{w_v}) - \arg(\tilde{\gamma}_{w_s})}{k_z} + \varepsilon\frac{\pi}{k_z}\left(1 - \frac{2 \cdot \sin^{-1}(|\gamma_v|^{0.8})}{\pi}\right) \tag{10}$$

In this equation, ε is the weight factor, used to adjust the contribution levels of phase and amplitude information to the inversion results. The theoretical basis of this method is that phase information contains rich height information, but there is uncertainty in the determination of the phase center position; meanwhile, amplitude information (coherence) can reflect the intensity characteristics of forest scattering. Through the optimal selection of

the weight factor, an optimal balance can be found between the two types of information, thereby improving the inversion accuracy and robustness.

3.4. Accuracy Verification and Results Evaluation

The accuracy of the forest height inversion results obtained from each model was evaluated using statistical regression analysis. To comprehensively evaluate the inversion performance of each model, this study adopts the following main evaluation indicators: (1) Root Mean Square Error (RMSE) (Equation (11)), used to quantify the average magnitude of the difference between predicted values and observed values; (2) Coefficient of Determination R^2 (Equation (12)), used to evaluate the degree of correlation between inversion results and observed values. RMSE reflects the absolute error level of the inversion accuracy, where a smaller value indicates higher inversion accuracy; R^2 reflects the degree of linear correlation between the inversion results and the observed values, where a value closer to 1 indicates a better inversion effect. The combination of these two indicators can comprehensively evaluate the performance of each inversion model.

$$\mathrm{RMSE} = \sqrt{\frac{1}{n}\sum_{i=1}^{n}(Y_i - y_i)^2} \tag{11}$$

$$R^2 = 1 - \frac{\sum_{i=1}^{n}(y_i - \overline{y})^2}{\sum_{i=1}^{n}(Y_i - \overline{y})^2} \tag{12}$$

4. Results and Analysis

4.1. Inversion Performance Analysis of Simulated Forest Scenes

4.1.1. Selection of Simulated Scenes for Three Dominant Scattering Mechanisms

Freeman–Durden three-component decomposition was applied to simulated P-band PolInSAR forest data at varying resolutions to systematically examine changes in the relative contributions of each scattering mechanism as a function of resolution. Three resolutions—1, 3, and 4 m—were selected, corresponding to forest scenarios dominated by volume, double-bounce, and surface scattering, respectively. The relative contributions of each scattering mechanism in forested regions at these resolutions are presented in Table 2.

Table 2. Contribution proportions of each scattering mechanism at different resolutions.

Resolution (m)	Surface Scattering	Double-Bounce Scattering	Volume Scattering
1	0.22	0.1	0.64
3	0.17	0.45	0.35
4	0.39	0.26	0.34

Based on the three simulated forest scenes described above, this study applies four classical forest height inversion methods—the polarimetric phase center height estimation method, the complex coherence phase center differencing algorithm, the coherence amplitude inversion method, and the hybrid inversion method using both phase and coherence information—to retrieve forest height. Through comparative analysis of the inversion accuracy of each method under conditions dominated by different scattering mechanisms, the scattering mechanism adaptability of the four methods is evaluated, providing a quantitative basis for selecting the optimal inversion approach for different scattering regimes. The inversion results from the four methods are shown in Figure 6.

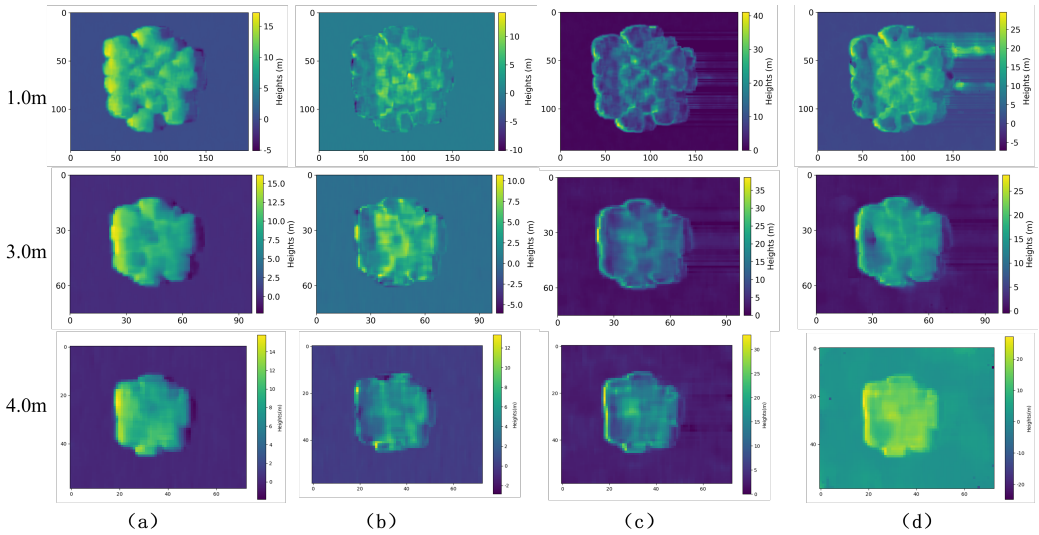


Figure 6. P-band inversion results: (**a**) polarimetric phase center height estimation method; (**b**) complex coherence phase center differencing algorithm; (**c**) coherence amplitude inversion method; (**d**) hybrid inversion method using both phase and coherence information.

4.1.2. Performance Evaluation of Four Inversion Methods in Simulated Data

To systematically evaluate the performance of the four inversion methods under different scattering conditions, this study uses the Root Mean Square Error (RMSE) between the retrieved forest heights and the prescribed true values as the quantitative evaluation metric. Table 3 presents the RMSE statistics for the four inversion methods under three dominant scattering mechanisms: volume scattering, double-bounce scattering, and surface scattering. The results reveal significant performance variations among the methods under different scattering regimes, providing a quantitative basis for selecting the appropriate inversion method for specific scattering conditions.

Table 3. Root Mean Square Error (RMSE) of Inversion Results for Four Forest Height.

Scene Parameters (m)	Polarimetric Phase Center Height Estimation Method	Complex Coherence Phase Center Differencing Algorithm	Coherence Amplitude Inversion Method	Hybrid Inversion Method Using Both Phase and Coherence Information
1	12.7068	13.7471	5.2642	5.3939
3	10.3242	12.8319	5.3037	3.267
4	9.9217	12.8776	3.6098	2.7853

As shown in Table 3, under P-band volume scattering dominance, the coherence amplitude inversion method achieves the highest accuracy, with an RMSE of 5.2642 m, significantly outperforming the other methods. In contrast, under surface scattering and double-bounce scattering dominance, the hybrid inversion method using both phase and coherence information exhibits superior performance, with RMSE of 2.7853 m and 3.267 m, respectively, substantially lower than those of the other methods under the same conditions. The polarimetric phase center height estimation method and the complex coherence phase center differencing algorithm show relatively lower accuracies across all three scattering regimes, with consistently higher RMSE than both the coherence amplitude inversion method and the hybrid inversion method using both phase and coherence information, indicating systematic underestimation at P-band. These results demonstrate that the optimal inversion method is scattering-mechanism-dependent: the hybrid inversion method using both phase and coherence information performs best under double-bounce and surface scattering conditions, while the coherence amplitude inversion method shows a distinct advantage under volume scattering dominance. This performance variation directly

reflects the strong coupling between inversion method effectiveness and the dominant scattering mechanism.

Comprehensive analysis reveals that the hybrid inversion method using both phase and coherence information demonstrates superior inversion performance when surface scattering and double-bounce scattering are dominant, exhibiting strong adaptability across different scattering conditions. Meanwhile, the aforementioned analysis further reveals an important phenomenon: a significant coupling effect exists between each inversion method and the scattering mechanism. That is, the same inversion method exhibits obvious performance differences under different dominant scattering mechanism conditions, and no single method possesses an absolute advantage under all scattering conditions. This understanding holds important guiding significance for the subsequent selection and optimization of inversion methods. However, the above conclusions are based only on idealized simulated data. In simulated data, relevant forest parameters (such as density and tree height) are set with a relatively uniform spatial distribution, whereas actual forests possess significant spatial heterogeneity. Therefore, to fully demonstrate the guiding value of this conclusion, further verification combined with real-world data is required.

4.2. Inversion Performance Analysis of Airborne PolInSAR Real Data

4.2.1. Distribution Characteristics of Dominant Scattering Mechanisms in the Study Area

Given that simulated data possess highly idealized characteristics while real forest areas involve numerous variables, this paper further utilizes P-band BioSAR data to verify the performance of the four inversion methods under the dominance of different scattering mechanisms. To this end, this paper adopts the Freeman–Durden three-component polarimetric decomposition method to perform polarimetric decomposition on the airborne PolInSAR data and extract the corresponding dominant scattering mechanisms. Subsequently, the areas dominated by different scattering mechanisms are delineated through mask processing, and the four classical forest height inversion methods are respectively applied to retrieve forest height, thereby determining the preferred method under each dominant scattering mechanism. The spatial distribution of dominant scattering mechanisms in the P-band BioSAR data is shown in Figure 7.

4.2.2. Performance Evaluation of Four Inversion Methods Under Different Dominant Scattering Mechanisms

This section obtains the inversion results under different dominant scattering mechanisms by applying four classical forest height inversion methods (the polarimetric phase center height estimation method, the complex coherence phase center differencing algorithm, the coherence amplitude inversion method, and the hybrid inversion method using both phase and coherence information) to the BioSAR airborne PolInSAR data, combined with the Freeman–Durden three-component polarimetric decomposition results. To systematically evaluate the methods' performance, this study uses LiDAR reference data for accuracy verification. Given the uneven distribution of sample points across different dominant scattering mechanisms, a spatial stratified random sampling strategy was employed in this study to ensure the statistical representativeness of the validation and to effectively mitigate sampling bias. Specifically, the regions characterized by the three dominant scattering mechanisms were treated as independent sampling strata, and 150 sample points were randomly selected within each category to evaluate the accuracy of individual inversion models. Meanwhile, to assess the global inversion performance of the joint inversion method, the collection of 450 sample points obtained through the aforementioned stratified sampling was aggregated for global accuracy validation. The spatial distribution of the accuracy validation sample points is illustrated in Figure 8.

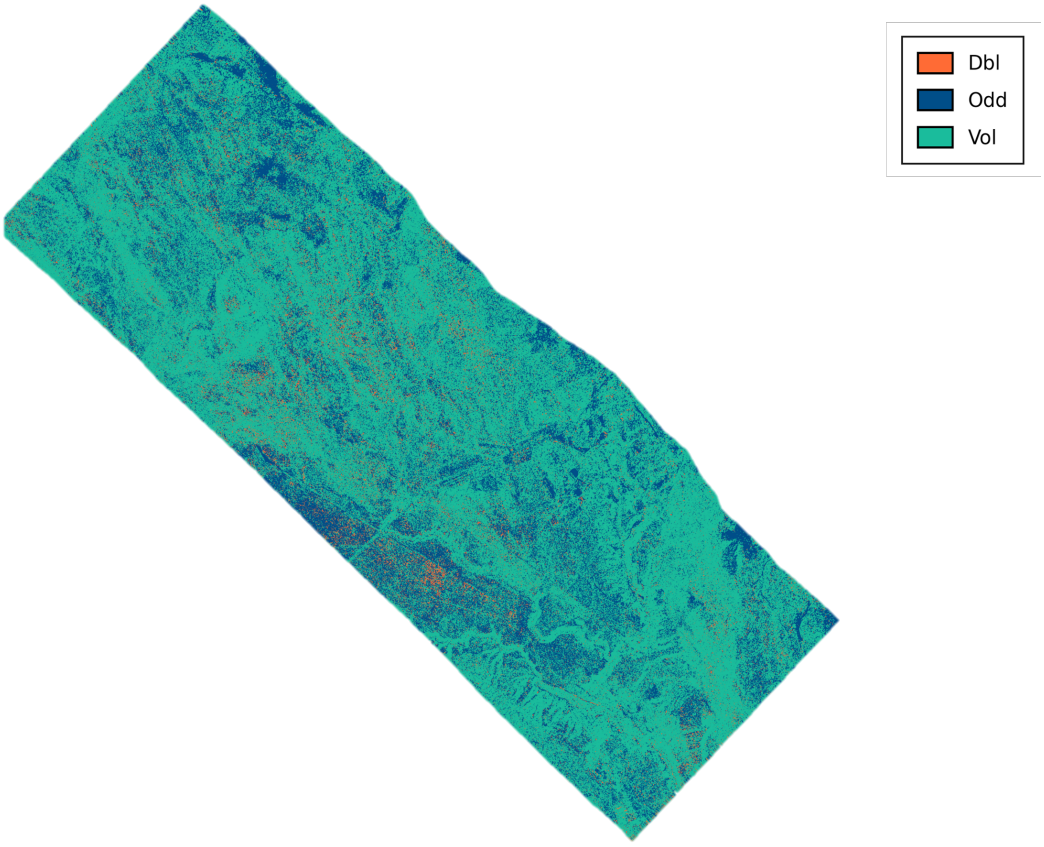


Figure 7. Schematic diagram of dominant distribution areas of different scattering mechanisms.

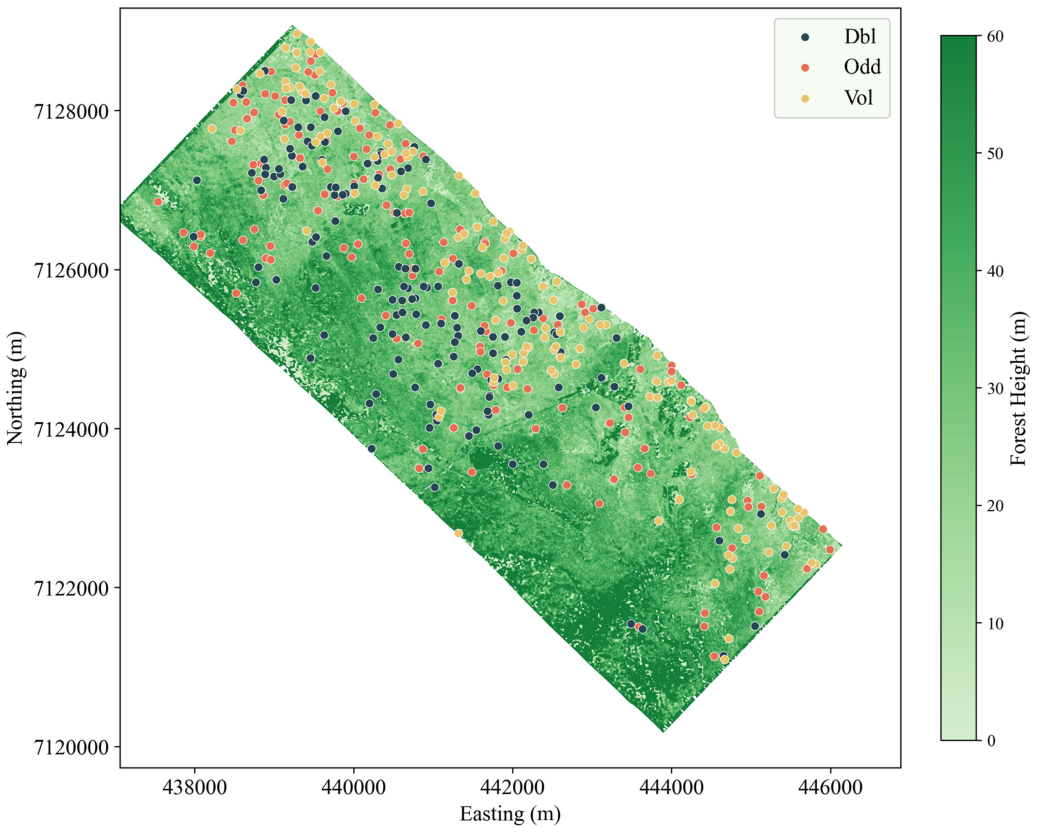


Figure 8. Distribution of sample points.

In the P-band, when surface scattering is dominant, the inversion performance of the four methods differs significantly (as shown in Figure 9). Among them, the hybrid inversion method using both phase and coherence information (Figure 9a) demonstrates optimal performance, with an RMSE of 6.16 m and an R^2 of 0.4948, and its scatter distribution is the most compact and closest to the 1:1 reference line. Although the coherence amplitude inversion method (Figure 9c) has the highest correlation (R^2 = 0.6440), its RMSE is as high as 12.59 m, indicating that while this method can capture height variation trends, it suffers from severe systematic underestimation due to the failure to effectively suppress interference. The polarimetric phase center height estimation method (Figure 9d) is affected by the strong penetration capability of the P-band, causing the phase center to shift downward toward the ground; its R^2 is only 0.4046, and the scatter distribution is extremely discrete, failing to effectively reflect the canopy height. The complex coherence phase center differencing algorithm (Figure 9b) shows moderate performance (RMSE = 7.21 m) but still exhibits obvious underestimation in taller forest areas. Overall, the hybrid inversion method using both phase and coherence information possesses the highest accuracy and robustness in scenes dominated by surface scattering at P-band.

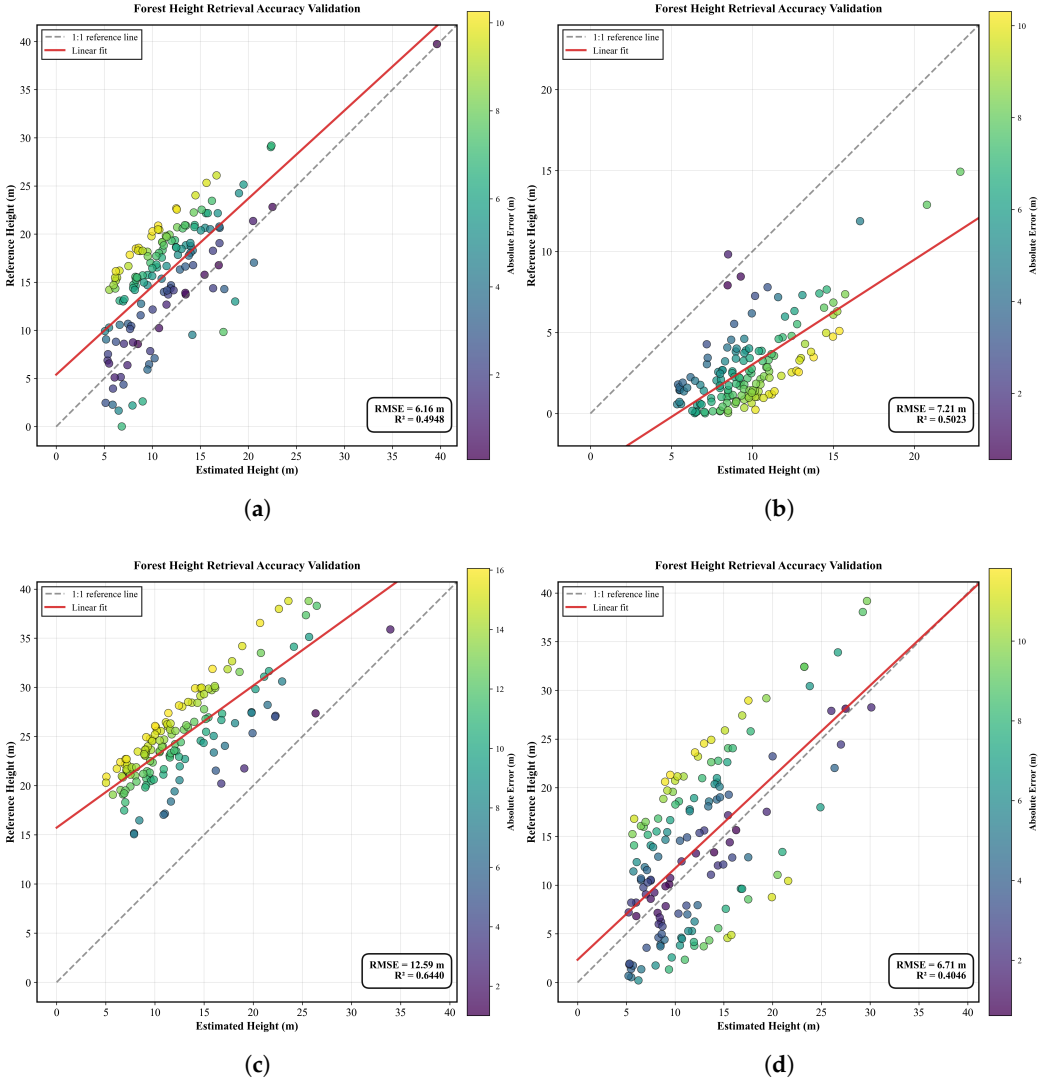


Figure 9. Scatter plots of accuracy verification for four inversion methods when surface scattering is dominant in P-band: (**a**) hybrid inversion method using both phase and coherence information; (**b**) complex coherence phase center differencing algorithm; (**c**) coherence amplitude inversion method; (**d**) polarimetric phase center height estimation method.

Under the dominance of double-bounce scattering (F_Dbl) at P-band, the accuracy performance of the four inversion methods is shown in Figure 10. The hybrid inversion method using both phase and coherence information (Figure 10a) still demonstrates the strongest applicability, with an RMSE of 6.49 m and an R^2 of 0.4711, and its scatter distribution is compact, with a high degree of agreement with the 1:1 reference line. In contrast, although the coherence amplitude inversion method (Figure 10c) exhibits the highest correlation (R^2 = 0.5213), its RMSE is as high as 13.55 m, reflecting that this method has a severe systematic underestimation bias when processing double-bounce scattering signals at P-band. The polarimetric phase center height estimation method (Figure 10d) and the complex coherence phase center differencing algorithm (Figure 10b) show poor inversion performance, with their R^2 both lower than 0.3 and extremely high scatter dispersion. This indicates that due to the extremely strong penetration capability of P-band, the double-bounce scattering path (ground-trunk interaction) is more severely affected by complex ground environments and non-structural noise, leading to insufficient robustness in height retrieval for methods relying solely on phase information.

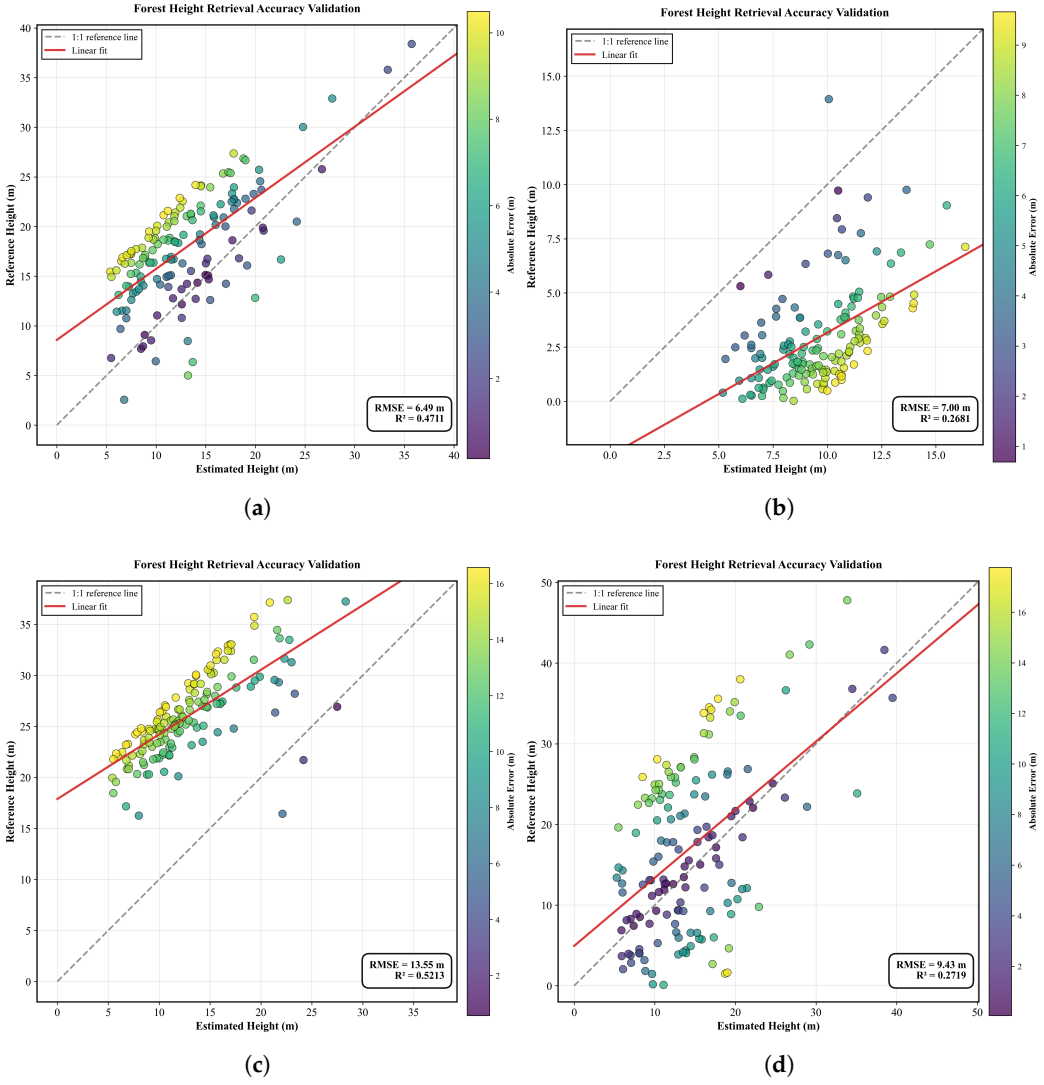


Figure 10. Scatter plots of accuracy verification for four inversion methods when double-bounce scattering is dominant in P-band: (**a**) hybrid inversion method using both phase and coherence information; (**b**) complex coherence phase center differencing algorithm; (**c**) coherence amplitude inversion method; (**d**) polarimetric phase center height estimation method.

At P-band, when volume scattering is dominant (Figure 11), the performance of each inversion method exhibits clear stratification. The coherence amplitude inversion method (Figure 11c) demonstrates the strongest linear correlation in this scene, with an R^2 reaching 0.7613 and an RMSE of only 5.36 m, reflecting that this method has high adaptability in modeling polarimetric interferometric echoes where volume scattering prevails. The hybrid inversion method using both phase and coherence information (Figure 11a) still maintains robust inversion accuracy, with an RMSE of 6.13 m and an R^2 of 0.5782, and its scatter distribution is compact and fits the 1:1 reference line well. In contrast, the polarimetric phase center height estimation method (Figure 11d) and the complex coherence phase center differencing algorithm (Figure 11b) perform poorly, with their R^2 values being only 0.1524 and 0.3040 respectively, and the scatter distributions are extremely discrete, with severe underestimation. This indicates that at P-band with stronger penetration capability, because the volume scattering process is more complex and susceptible to interference from underlying ground echoes, methods relying solely on phase information struggle to obtain stable inversion accuracy in volume scattering dominant areas, whereas methods incorporating amplitude information can better capture the vertical scattering characteristics of the forest canopy.

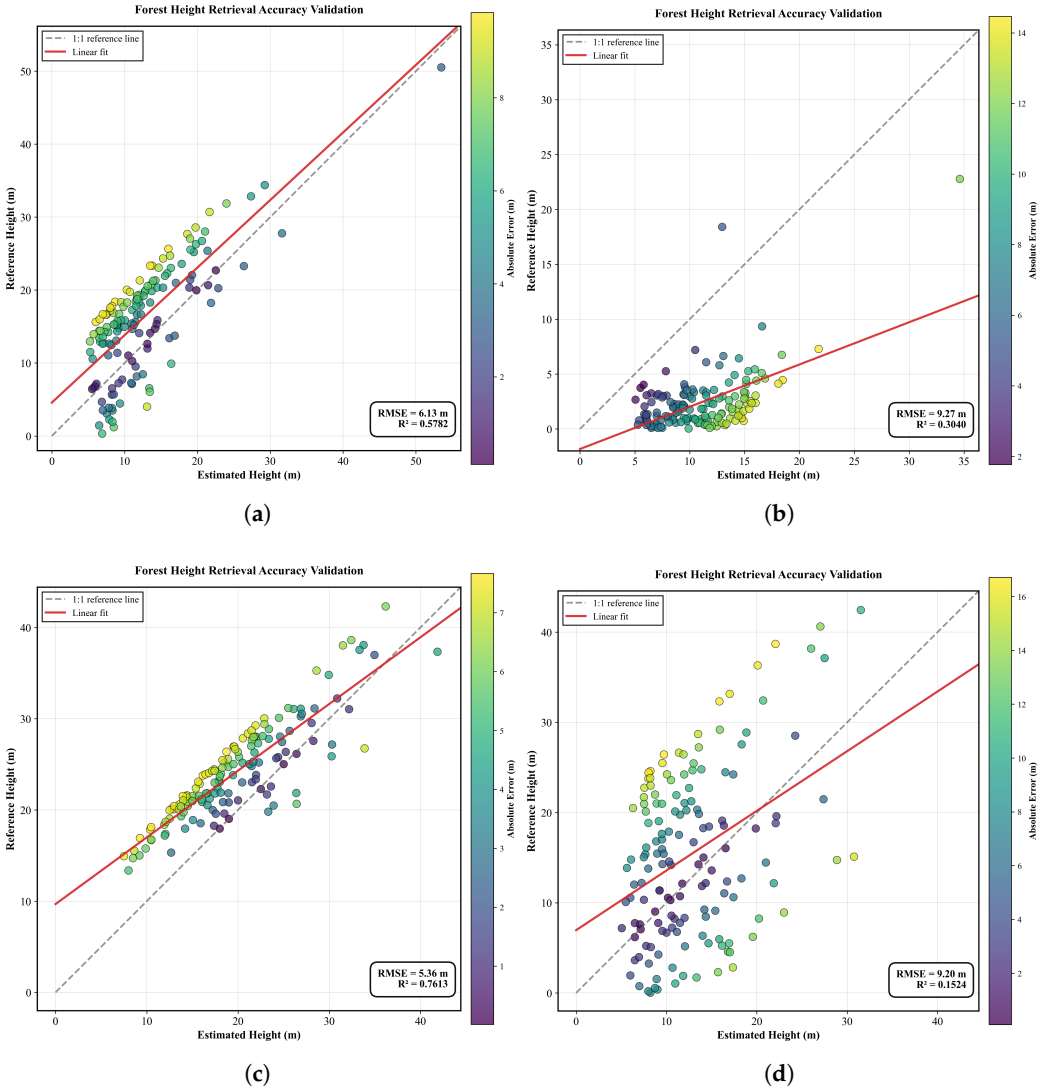


Figure 11. Scatter plots of accuracy verification for four inversion methods when volume scattering is dominant in P-band: (**a**) hybrid inversion method using both phase and coherence information; (**b**) complex coherence phase center differencing algorithm; (**c**) coherence amplitude inversion method; (**d**) polarimetric phase center height estimation method.

In summary, the effectiveness and performance of each inversion method at P-band exhibit a significant coupling relationship with the dominant scattering mechanisms. Specifically, in scenes where surface scattering and double-bounce scattering are dominant, the hybrid inversion method using both phase and coherence information demonstrates superior inversion performance through the comprehensive utilization of various scattering information. Conversely, in volume scattering dominant areas, the coherence amplitude inversion method shows better applicability. This pattern is consistent with the inversion performance of each method in the simulated data and has been verified through real data, indicating that this coupling relationship possesses a certain degree of stability and predictability. The underlying reason for this coupling phenomenon lies in the physical penetration characteristics of the P-band and the resulting direct impact of canopy–ground interactions on the theoretical assumptions of different algorithms. The long wavelength of the P-band endows it with exceptionally strong electromagnetic wave penetration capabilities. Specifically, in regions dominated by volume scattering, although the P-band can penetrate the canopy, the radar waves undergo multiple reflections with branches and trunks within the forest during propagation due to the complexity of the internal forest structure, thereby forming volume scattering signals. Under this physical premise, the complex coherence amplitude inversion method directly utilizes the amplitude characteristics of the electromagnetic waves within the canopy for inversion. This effectively avoids the inversion instability caused by the low separability of polarimetric phase centers in dense forest canopies, thus demonstrating better theoretical applicability. Conversely, in scenarios dominated by surface scattering and dihedral scattering, the long wavelength allows radar waves to penetrate the forest canopy and reach the ground surface. In this case, the phase center is close to the ground, and relying solely on the phase center method would severely underestimate the forest height. On the other hand, methods based on coherence primarily characterize canopy scattering, which tends to overestimate the forest height to a certain extent. In such situations, the coherence amplitude and phase combined inversion method integrates both phase and amplitude information, allowing the two to compensate for each other, thereby effectively improving the estimation accuracy of forest height.

Notably, by comparing the inversion results between the simulated and real data, it is observed that both exhibit a high degree of consistency regarding the selection of the optimal method under various scattering conditions. This indicates that the relationship between the methods and scattering mechanisms established under simulated conditions possesses a certain degree of transferability, meaning that it remains applicable in actual forest scenarios. Meanwhile, this consistency also reveals a crucial phenomenon: different inversion models exhibit distinct preferences for specific scattering mechanisms, making it difficult for a single model to maintain optimal performance across all scenarios. However, although both exhibit consistent trends in performance evolution, a certain gap remains in the overall inversion accuracy under real data scenarios compared to idealized simulated scenarios. This accuracy discrepancy primarily stems from forest heterogeneity within real forest ecosystems, including the diversity of tree species, variations in stand density, and topographic undulations. Secondly, the structural complexity of the canopy in real forest scenarios also introduces significant deviations from simulated environments. Finally, real airborne PolInSAR data are inevitably affected by sensor and environmental noise, as well as temporal decorrelation, which further increases model fitting errors. In summary, it is precisely the complexity of real-world environments that limits the global-scale accuracy performance of single inversion models. For these reasons, selecting an inversion model that matches specific dominant scattering mechanism conditions becomes particularly necessary. Furthermore, exploring an adaptive joint inversion strategy driven by dominant scattering mechanisms can effectively overcome the interference of these complex real-

istic factors, demonstrating tremendous potential to significantly enhance global overall inversion accuracy and robustness.

4.3. Adaptive Inversion Fusion Based on Dominant Scattering Mechanisms

To verify the practical application value of the aforementioned methods, this paper further applies an adaptive combined inversion strategy based on dominant scattering mechanisms at P-band. Figure 12 displays the forest height inversion map generated by the combined strategy (e) and the forest height maps generated under single inversion methods (a–d). Figure 13 compares the accuracy differences between the combined strategy and the single methods. Table 4 further presents the statistical evaluation results (95% confidence intervals) based on the validation samples.

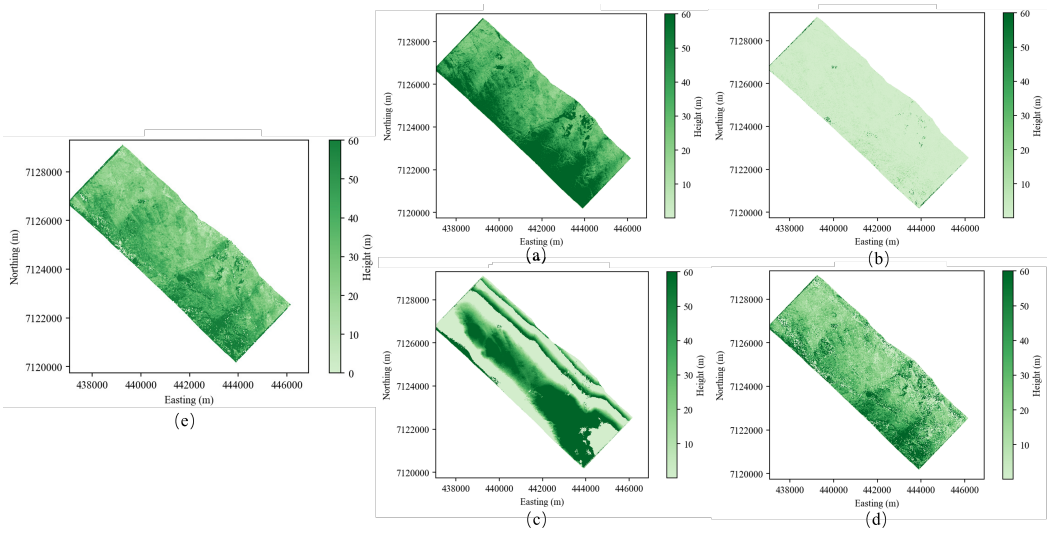


Figure 12. P-band inversion results: (**a**) coherence amplitude inversion method; (**b**) complex coherence phase center differencing algorithm; (**c**) polarimetric phase center height estimation method; (**d**) hybrid inversion method using both phase and coherence information; (**e**) combined inversion method.

Experimental data show that the adaptive combined inversion strategy demonstrates outstanding performance at P-band, significantly outperforming all single PolInSAR inversion methods. Firstly, from the perspective of the algorithms' intrinsic performance, when comparing the overall inversion accuracy of all algorithms without differentiating scattering mechanisms, the optimal single model (the coherence amplitude and phase combined inversion method) yielded an RMSE of 6.51 m across the global remote sensing imagery (with a 95% confidence interval of [6.25, 6.75]). Because the single method fails to fully account for the spatial heterogeneity of forest scattering mechanisms, it still generates significant local deviations when applied to non-dominant scattering regions. In contrast, the joint inversion method proposed in this paper increases the global R^2 to 0.7622 and reduces the RMSE to 4.62 m (with a 95% confidence interval of [4.47, 4.77] m). This error reduction of approximately 30% can be explicitly attributed to the 'adaptive joint algorithm driven by dominant scattering mechanisms' proposed in this study. This result clearly elucidates that while the best-performing single algorithm lays the performance foundation for inversion algorithms, the adaptive inversion based on dominant scattering mechanisms serves as the core driving force to break through the bottleneck of single models and achieve the ultimate leap in global forest height inversion performance.

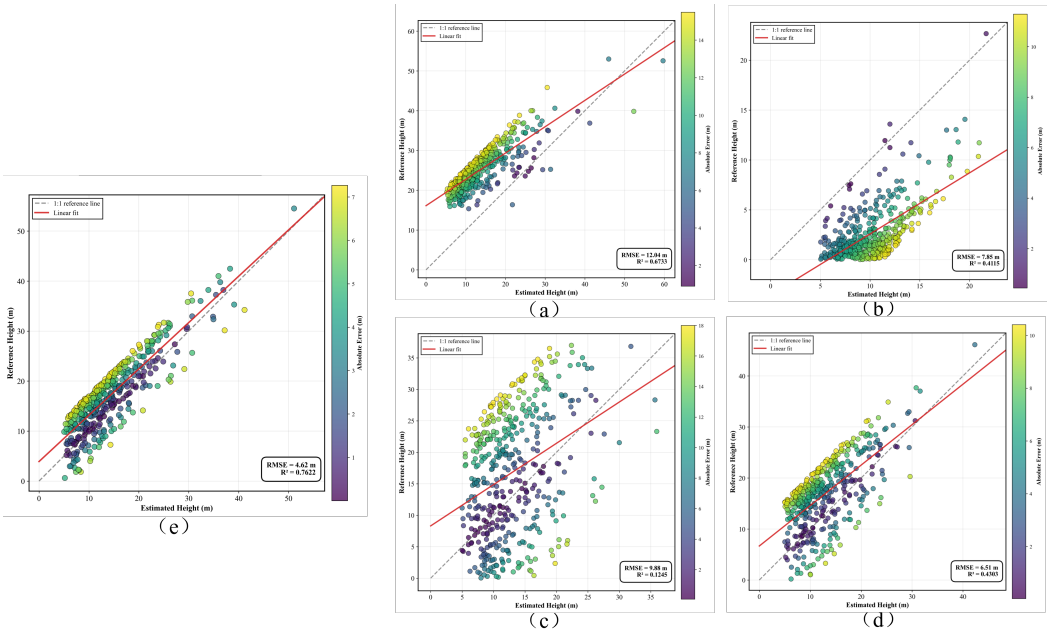


Figure 13. Accuracy verification plots for P-band: (**a**) coherence amplitude inversion method; (**b**) complex coherence phase center differencing algorithm; (**c**) polarimetric phase center height estimation method; (**d**) hybrid inversion method using both phase and coherence information; (**e**) combined inversion method.

Table 4. Accuracy and 95% confidence intervals of different inversion models based on the global validation samples.

Inversion Model	RMSE (m)	95% Confidence Interval (m)	Coefficient of Determination (R^2)
Coherence amplitude inversion method	12.04	[11.80, 12.31]	0.6733
Complex coherence phase center differencing algorithm	7.85	[7.65, 8.03]	0.4115
Polarimetric phase center height estimation method	9.88	[9.42, 10.35]	0.1245
Hybrid inversion method using both phase and coherence information	6.51	[6.25, 6.75]	0.4303
Combined inversion method	4.62	[4.47, 4.77]	0.7622

In summary, at P-band, the variation in dominant scattering mechanisms has a significant impact on the forest height estimation of different inversion algorithms, and it is difficult for a single method to maintain optimal performance across the entire scene. The patterns discovered in the simulated data—specifically, that the hybrid inversion method using both phase and coherence information performs better when surface scattering and double-bounce scattering are dominant, while the coherence amplitude inversion method performs better when volume scattering is dominant—have been verified in the real data validation, demonstrating a certain degree of stability. Based on this understanding, this study further explored strategies for selecting or fusing the optimal inversion method according to the dominant scattering mechanisms. Preliminary results indicate that this adaptation strategy based on physical mechanisms, compared to a single method, can maintain better inversion performance under a wider range of scattering conditions, providing a feasible technical path for improving the accuracy of global forest height inversion.

Through the identification of physical mechanisms and the complementary advantages of methods, this approach provides a promising technical solution for the extraction of forest height parameters and holds certain guiding significance for research on P-band PolInSAR forest height inversion.

5. Discussion

This paper systematically analyzes the performance of four inversion methods using P-band PolInSAR data under different dominant scattering mechanisms and, based on this, proposes an adaptive combined inversion strategy based on dominant scattering mechanisms. The research results further reveal the deep coupling relationship between inversion method performance and scattering mechanisms, a finding that aligns well with and complements existing research.

5.1. Coupling Relationship Between Scattering Mechanisms and Inversion Model Performance

Existing studies have highlighted the limitations of using a single inversion method in complex forest scenarios. In a review of PolInSAR forest height inversion techniques, Xing et al. [31] pointed out that while RVoG-based inversion methods possess a solid theoretical foundation, their effectiveness largely depends on whether the forest scattering patterns conform to the model assumptions. Although the three-stage inversion algorithm is widely applied, it still faces challenges in accurately estimating ground scattering contributions when dealing with complex scattering conditions. Simultaneously, Wang et al. [32], in proposing the Time–Frequency RVoG model, particularly emphasized the necessity of accurately identifying surface, double-bounce, and volume scattering mechanisms via multi-component decomposition. Their research indicated that the accurate identification of scattering mechanisms is a key prerequisite for improving forest height inversion accuracy. The aforementioned studies suggest that a deep coupling relationship exists between scattering mechanisms and method inversion accuracy during the forest height inversion process. The analysis of P-band data in this study further confirms this finding. P-band radar waves possess strong penetration capabilities, resulting in echo signals that contain significant complex double-bounce scattering information formed by interactions between the ground and tree trunks. However, the traditional three-stage inversion algorithm is typically based on a key assumption: that there exists at least one polarization channel in the observed data where the ground scattering contribution is negligible (i.e., the ground-to-volume scattering ratio is close to zero), thereby implying that the decorrelation in that channel originates primarily from volume scattering [33]. In the P-band double-bounce dominant region, strong double-bounce scattering generated by ground-trunk interactions violates this “pure volume scattering” assumption, leading to a significant degradation in forest height inversion accuracy. The results of this study further validate the significant dependence of method performance on scattering mechanisms across different inversion algorithms, thereby establishing the necessity of distinguishing dominant scattering mechanisms and treating them distinctively.

5.2. Physical Mechanism and Advantages of Adaptive Combined Inversion

Single methods struggle to adapt to the global variations in scattering mechanisms. Lin et al. [34] found in multi-baseline PolInSAR inversion studies that the traditional three-stage method exhibits serious inversion bias under specific conditions, whereas an improved multi-baseline inversion scheme could increase accuracy by 26%. This possesses intrinsic consistency with the findings of this study, namely that a single inversion method is difficult to adapt to the variations in global scattering mechanisms to obtain high-precision forest height estimation. Based on this, the adaptive strategy proposed in

this study, through explicit mechanism identification, constructs a combined inversion approach based on dominant scattering mechanisms, thereby improving inversion accuracy in complex forest scenarios. However, unlike existing multi-method weighted fusion approaches, the mechanism-driven strategy adopted in this study possesses a clearer physical orientation. Although weighted methods can statistically reduce inversion errors, they cannot fundamentally eliminate the systematic bias caused by the misjudgment of scattering mechanisms. By partitioning the study area into different scattering-dominant regions using polarimetric decomposition, this strategy essentially applies the inversion method capable of retrieving the most relatively correct forest height information within each sub-region. Experimental results indicate that the RMSE in the combined inversion strategy is significantly reduced, confirming the superiority of this strategy when processing P-band PolInSAR data for forest height inversion. Furthermore, with the advancement of the European Space Agency (ESA) BIOMASS satellite mission, the application of P-band spaceborne radar data will become increasingly prevalent. However, given that spaceborne platforms are more significantly affected by revisit cycles and temporal decorrelation, the aliasing effects of their scattering mechanisms will be more complex than those in airborne data. In coping with such complex mixed scattering conditions, variations in spatial resolution, or high system noise, the Freeman–Durden polarimetric decomposition method currently relied upon by this framework exhibits certain sensitivities and limitations. The errors originating from this polarimetric decomposition stage propagate through the adaptive decision mechanism constructed in this study, leading to deviations in the classification of dominant scattering mechanisms and model selection, which subsequently introduces systematic biases in forest height estimation. Despite the method's high dependence on the initial decomposition accuracy, the mechanism-based adaptive inversion framework validated in this study still provides a transferable a priori knowledge framework for forest parameter inversion using future spaceborne P-band data. In future research, to further enhance the robustness of this framework in extremely complex environments, the introduction of other polarimetric decomposition techniques as alternative or synergistic solutions could be considered. For instance, methods such as Yamaguchi decomposition, H/α decomposition, Cloude–Pottier decomposition, and other advanced polarimetric decomposition techniques could be integrated to significantly enhance the robustness against system noise and improve the overall stability of the inversion method.

6. Conclusions and Future Work

Through validation using both simulated data and real airborne PolInSAR data, this paper draws the following main conclusions. (1) The performance of different forest height inversion methods is deeply coupled with the dominant scattering mechanisms of the forest area. In regions dominated by surface and double-bounce scattering, the hybrid inversion method using both phase and coherence information exhibits superior performance, whereas in regions dominated by volume scattering, the coherence amplitude inversion method demonstrates better performance. Significantly, this correspondence established in the simulated data is fully corroborated in the real PolInSAR data, indicating that this pattern possesses strong stability and universality in P-band forest parameter inversion. (2) The adaptive strategy proposed in this study significantly improves global inversion accuracy. It effectively resolves the limitation that single methods struggle to accommodate the global scattering characteristics of complex forest areas. Experimental results indicate that the proposed adaptive combined inversion strategy achieves a substantial improvement in accuracy: the Root Mean Square Error (RMSE) is reduced from 6.51 m (the best performance among single methods) to 4.62 m, and the coefficient of determination (R^2) is increased from 0.4303 to 0.7622. In contrast, traditional studies mostly employ single

inversion methods, which often have limited generalization capabilities. This approach not only provides a new technical pathway for height inversion in complex forest areas but also offers core technical support for subsequent precise estimation of forest carbon stocks and biomass monitoring.

Although the adaptive inversion strategy proposed in this study has demonstrated significant advantages in P-band forest height estimation, its generalization capability and practical application potential across broader scenarios warrant further exploration. Firstly, during the dominant scattering mechanism identification stage, the current framework relies on a relatively singular polarimetric decomposition method. In future research, diverse polarimetric target decomposition techniques should be introduced to more accurately address the scattering characteristics in complex forest areas, thereby improving the robustness of dominant scattering mechanism extraction. Secondly, this study primarily focuses on P-band BioSAR data from specific forest regions in Sweden. If this method is extended to different forest types (such as tropical rainforests or mixed broadleaf forests), the extremely high biomass, complex tree species distribution, and high canopy closure in these regions will significantly affect the penetration of microwave signals through the canopy. This, in turn, will impact the accurate identification of dominant scattering mechanisms and the precision of the inversion algorithms. Therefore, subsequent research should focus on evaluating the specific performance and applicability of this method under such complex forest structures. Finally, regarding radar bands, the selection of the adaptive algorithm is highly dependent on the penetration characteristics of the electromagnetic waves. Unlike the robust canopy penetration capability of the P-band, the shorter wavelengths of L-band or C-band data result in substantially weakened penetration. Consequently, the radar signals will primarily originate from the middle and upper layers of the forest canopy, and the contribution of surface scattering will be significantly reduced. Therefore, future research could attempt to combine the deeply penetrating P-band with L/C-band data—which possess canopy detail characterization capabilities—alongside high-resolution optical and LiDAR data. By leveraging the physical complementarity of multi-source data, a more universally applicable forest structural parameter inversion model could be constructed to comprehensively address the dynamic monitoring demands of various climate zones and complex forest types globally.

Author Contributions: Conceptualization, F.D., W.Z., Y.J. and H.Z.; methodology, F.D. and H.Z.; validation, F.D.; formal analysis, F.D.; resources, W.Z. and Y.J.; data curation, F.D.; writing—original draft preparation, F.D.; writing—review and editing, W.Z. and Y.J.; visualization, F.D.; supervision, W.Z. and Y.J. All authors have read and agreed to the published version of the manuscript.

Funding: This research was funded by the National Natural Science Foundation of China (grant numbers 32371869, 42161059, 32471865, 32160365, and 31860240); Yunnan Fundamental Research Projects (grant number 202401BB070001-021); Key Laboratory for Forest Resources Conservation and Utilization in the Southwest Mountains of China, Ministry of Education; Key Laboratory for Conservation and Utilization of In-forest Resource of Yunnan; and Key Laboratory of Forest Disaster Warning and Control in Yunnan Province (grant number LXXK-2025D19).

Data Availability Statement: The datasets used in this study are available from the corresponding author upon reasonable request.

Acknowledgments: The authors would like to thank their supervisors for their guidance and support throughout this research. We also extend our sincere gratitude to the editors and anonymous reviewers for their time and constructive comments, which have significantly improved the quality of this manuscript.

Conflicts of Interest: The authors declare no conflicts of interest.

References

1. Wan, J.; Wang, C.C.; Zhu, J.J.; Fu, H.Q. Research progress on tomographic SAR three-dimensional imaging ethods and forest parameter inversion. *Natl. Remote Sens. Bull.* **2024**, *28*, 576–590.
2. Hu, T.Y.; Liu, X.Q.; Wu, X.Y.; Niu, C.Y.; Su, Y.J. Advance in forest canopy structural complexity research. *Natl. Remote Sens. Bull.* **2025**, *29*, 83–101.
3. Li, Z.Y.; Zhao, L.; Li, K.; Chen, E.X.; Wan, X.X.; Xu, K.P. A survey of developments on forest resources monitoring technology of synthetic aperture radar. *J. Nanjing Univ. Inf. Sci. Technol. Nat. Sci. Ed.* **2020**, *12*, 150–158.
4. Zhu, J.J.; Xie, Y.Z.; Fu, H.Q.; Wang, C.C. Penetration Mapping of Forest Cover Using Spaceborne P-Band SAR: A Review of the European Space Agency's BIOMASS Mission. *Geomat. Inf. Sci. Wuhan Univ.* **2025**, *50*, 1457–1468.
5. Lu, D.S.; Jiang, X.D.; Li, Y.H.; Wang, R.Q.; Li, G.Y. Forest biomass estimation with LiDAR data. *Natl. Remote Sens. Bull.* **2025**, *29*, 2035–2064.
6. Neumann, M.; Saatchi, S.S.; Ulander, L.M.H.; Fransson, J.E.S. Assessing Performance of L- and P-Band Polarimetric Interferometric SAR Data in Estimating Boreal Forest Above-Ground Biomass. *IEEE Trans. Geosci. Remote Sens.* **2012**, *50*, 714–726.
7. Wu, C.J.; Shen, P.; Tebaldini, S.; Yu, Y.H.; Liao, M.S. Forest Vertical Structure Inversion Based on Baseline Optimization InSAR Phase Histogram Technique. *Geomat. Inf. Sci. Wuhan Univ.* **2025**, *50*, 1608–1618.
8. Kumar, S. Advancing forest structure retrieval through multi-frequency PolInSAR and TomoSAR: Leveraging ESA's P-band Biomass and NASA–ISRO NISAR missions. *ISPRS Ann. Photogramm. Remote Sens. Spat. Inf. Sci.* **2025**, *X-5/W2-2025*, 341–349.
9. Zhang, Q.; Ge, L.L.; Hensley, S.; Metternicht, G.I.; Liu, C.; Zhang, R.H. PolGAN: A deep-learning-based unsupervised forest height estimation based on the synergy of PolInSAR and LiDAR data. *ISPRS J. Photogramm. Remote Sens.* **2022**, *186*, 123–139. [CrossRef]
10. Fan, W.J.; Peng, N.J.; Cao, B.; Mu, X.H.; Yang, S.Q.; He, Q.C.; Zhai, D.C.; Ren, H.Z.; Cui, Y.K.; Yan, G.J. Progress inhigh spatial resolution vegetation quantitative remote sensing. *Natl. Remote Sens. Bull.* **2025**, *29*, 1365–1387.
11. Li, Z.Y.; Chen, E.X.; Qin, X.L.; Guo, Y.; Tian, X.; Liu, Q.W.; Sun, B.; Zhao, L.; Cai, S.S.; Du, L.M.; et al. Research and application of forestry and grassland remote sensing technology in China: Recent progress, challenges and countermeasures. *Natl. Remote Sens. Bull.* **2025**, *29*, 1804–1830.
12. Liu, X.; Neigh, C.S.R.; Pardini, M.; Forkel, M. Estimating forest height and above-ground biomass in tropical forests using P-band TomoSAR and GEDI observations. *Int. J. Remote Sens.* **2024**, *45*, 3129–3148. [CrossRef]
13. Xie, Y.; Fu, H.; Zhu, J.; Wang, C.C.; Xie, Q.H.; Wan, J.; Han, W.T. Improved forest height mapping using multibaseline low-frequency PolInSAR data based on effective selection of dual-baseline combinations. *Remote Sens. Environ.* **2024**, *312*, 114306. [CrossRef]
14. Zhang, T.W. Uncertainty Analysis in Forest Height Inversion Using Polarimetric SAR Interferometry Data. Master's Thesis, Southwest Forestry University, Kunming, China, 2021. (In Chinese)
15. Chen, Y. Research on the Forest Height Retrieval Based on Polarimetric and Interferometric Synthetic Aperture Radar. Master's Thesis, University of Electronic Science and Technology of China, Chengdu, China, 2021. (In Chinese)
16. Xue, C. Research on Vegetation Parameters Inversion Method of Single/Multi-Baseline PolInSAR. Master's Thesis, Xidian University, Xi'an, China, 2019. (In Chinese)
17. Zhang, W.F.; Chen, E.X.; Li, Z.Y.; Zhao, L.; Ji, Y.J. Development of Forest Height Estimation Using InSAR/PolInSAR Technology. *Remote Sens. Technol. Appl.* **2017**, *32*, 983–997.
18. Li, W.M. Forest Vertical Structure Parameters Estimation Using Polarimetric Interferometric Tomography SAR. Master's Thesis, Chinese Academy of Forestry, Beijing, China, 2013.
19. Chen, W.; Zheng, Q.H.; Xiang, H.B.; Chen, X.; Sakai, T. Forest Canopy Height Estimation Using Polarimetric Interferometric Synthetic Aperture Radar (PolInSAR) Technology Based on Full-Polarized ALOS/PALSAR Data. *Remote Sens.* **2021**, *13*, 174. [CrossRef]
20. Yadav, S.; Padalia, H.; Sinha, S.K.; Srinet, R.; Chauhan, P. Above-ground biomass estimation of Indian tropical forests using X band Pol-InSAR and Random Forest. *Remote Sens. Appl. Soc. Environ.* **2021**, *21*, 100462. [CrossRef]
21. Sui, A.; Michel, O.O.; Mao, Y.; Fan, W.Y. An Improved Forest Height Model Using L-Band Single-Baseline Polarimetric InSAR Data for Various Forest Densities. *Remote Sens.* **2023**, *15*, 81. [CrossRef]
22. Williams, M.L.; Pottier, E.; Ferro-Famil, L.; Allain, S.; Cloude, S.R.; Hajnsek, I.; Papathanassiou, K.; Moreira, A.; Minchella, A.; Desnos, Y.L. Forest coherent SAR simulation within PolSARPro: An educational toolbox for PolSAR and PolInSAR data processing. In Proceedings of the Asian Conference on Remote Sensing, Kuala Lumpur, Malaysia, 12–16 November 2007; Volume 6, pp. 55–74.
23. Fan, M.Y. Research on Forest Height Estimation from Polarimetric SAR Interferometry Images. Master's Thesis, Harbin Institute of Technology, Harbin, China, 2014. (In Chinese)
24. Zhang, T.W.; Ji, Y.J.; Zhang, W.F. The analysis on uncertainty resulting from method and wavelength selecting in forest height inversion using simulated polarimetric interferometric SAR data. *Natl. Remote Sens. Bull.* **2022**, *26*, 1963–1975.

25. Han, W.T.; Zhou, C.; Zhu, J.J.; Fu, H.Q.; Xie, Q.H.; Hu, J.; Wang, C.C.; Gao, H. Research Progress and Challenges in the PolSAR Decompositon. *Geomat. Inf. Sci. Wuhan Univ.* **2024**, *50*, 1498–1516.
26. Cloude, S.R.; Pottier, E. An Entropy Based Classification Scheme for Land Applications of Polarimetric SAR. *IEEE Trans. Geosci. Remote Sens.* **1997**, *35*, 68–78.
27. Freeman, A.; Durden, S.L. A Three-Component Scattering Model for Polarimetric SAR Data. *IEEE Trans. Geosci. Remote Sens.* **1998**, *36*, 963–973. [CrossRef]
28. Ji, Y.J.; Zhang, W.F.; Xu, K.P.; Ju, Y.L.; Li, W.; Jing, Q.; Wang, L.; Li, Y. Estimation of forest aboveground biomass based on GF-3 Quad-polarization SAR data. *Remote Sens. Technol. Appl.* **2023**, *38*, 362–371.
29. Song, G.P.; Wang, C.C.; Fu, H.Q.; Xie, Q.H. A Novel Vegetation Height Inversion Method Based on Polarimetric Interferometric Covariance Matrix Decomposition. *Acta Geod. Cartogr. Sin.* **2014**, *43*, 613–619, 636.
30. Yamaguchi, Y.; Moriyama, T.; Ishido, M.; Yamada, H. Four-Component Scattering Model for Polarimetric SAR Image Decomposition. *IEEE Trans. Geosci. Remote Sens.* **2005**, *43*, 1699–1706.
31. Xing, C.; Wang, H.M.; Zhang, Z.J.; Yin, J.J.; Yang, J. A Review of Forest Height Inversion by PolInSAR: Theory, Advances, and Perspectives. *Remote Sens.* **2023**, *15*, 3781.
32. Wang, L.; Zhou, Y.S.; Shen, G.Y.; Xiong, J.N.; Shi, H.T. Forest Height Inversion Based on Time-Frequency RVOG Model Using Single-Baseline L-Band Sublook-InSAR Data. *Remote Sens.* **2023**, *15*, 166.
33. Cloude, S.R.; Papathanassiou, K.P. Three-stage inversion process for polarimetric SAR interferometry. *IEE Proc.-Radar Sonar Navig.* **2023**, *150*, 125–134.
34. Lin, D.F.; Zhu, J.J.; Li, Z.Y.; Fu, H.Q.; Liang, J.; Zhou, F.B.; Zhang, B. A Multi-Baseline PolInSAR Forest Height Inversion Method Taking into Account the Model Ill-posed Problem. *J. Geod. Geoinf. Sci.* **2024**, *7*, 42–56.

Disclaimer/Publisher's Note: The statements, opinions and data contained in all publications are solely those of the individual author(s) and contributor(s) and not of MDPI and/or the editor(s). MDPI and/or the editor(s) disclaim responsibility for any injury to people or property resulting from any ideas, methods, instructions or products referred to in the content.